In situ x-ray diffraction study of dynamically compressed α-cristobalite using a dynamic diamond anvil cell

M. O. Schoelmerich [1,2,*] A. S. J. Mendez [3] C. Plueckthun [1] N. Biedermann,[1] R. Husband,[3] T. R. Preston [1] L. Wollenweber,[1] K. Klimm [4] T. Tschentscher [1] R. Redmer,[5] H. P. Liermann,[3] and K. Appel[1]

[1]*European XFEL GmbH, Schenefeld, 22869, Germany*
[2]*Lawrence Livermore National Laboratory, Livermore, California 94500, USA*
[3]*Deutsches Elektronen-Synchrotron DESY, Hamburg, 22607, Germany*
[4]*Goethe University Frankfurt, Frankfurt, 60438, Germany*
[5]*Universität Rostock, Institut für Physik, Rostock, 18051, Germany*

In this study we present results of the dynamic compression of α-cristobalite up to a pressure of 106 GPa with the use of the dynamic diamond anvil cell. X-ray diffraction images were recorded at different ramp compression and decompression rates to investigate *in situ* the high-pressure phase transitions of α-cristobalite. Our results suggest that the pressure onset of the phase transformation of α-cristobalite to cristobalite II, cristobalite X-I, and ultimately to seifertite (α-PbO$_2$ type SiO$_2$) is dependent on the applied compression rates and stress conditions of the experiment. Increasing compression rates in general shift the studied phase transitions to higher pressures. Furthermore, our results indicate for single crystals under hydrostatic conditions a suppression of a phase transition from cristobalite X-I to seifertite at pressures of up to 82 GPa.

I. INTRODUCTION

SiO$_2$ and its polymorphs have been widely investigated with respect to its structural behavior at high pressures and temperatures due to its importance in the field of geo and material sciences. Its high-pressure phase transformations, phase equilibria, and melting process are essential for understanding the interior structure and dynamic nature of planetary formation as well as impact phenomena. The high-pressure modifications of SiO$_2$ have therefore been extensively studied and a large number of theoretical predicted silica structures have been experimentally confirmed [1–11]. At temperatures exceeding 1470 °C and ambient pressures, SiO$_2$ crystallizes in the cubic β-cristobalite structure and, upon cooling to temperatures below ∼250 °C, transforms to tetragonal α-cristobalite (space group $P4_12_12$). In nature, the high-temperature SiO$_2$ polymorph can be found in volcanic rocks or ashes [12–14] and is a predominant SiO$_2$ constituent in meteorites [15]. Although α-cristobalite is an ambient pressure polymorph of SiO$_2$, it has been observed in meteorites within close spatial relation to high pressure minerals that show signatures of peak shock pressures exceeding 25 GPa [16–19]. In particular seifertite, the post-stishovite high-pressure polymorph of SiO$_2$, was found in proximity to α-cristobalite [17–20]. Such a vicinity of high- and low-pressure SiO$_2$ polymorphs indicates a complex pressure and temperature impact history, in which pressure increase, release, and cooling alters the mineral assemblages. It was experimentally shown, that α-cristobalite undergoes several phase transitions at high pressures. It transforms from tetragonal α-cristobalite to monoclinic cristobalite II ($P2_1/c$) at ∼1.5 GPa and transits to the monoclinic cristobalite X-I structure ($P2_1/n$) at ∼11 GPa [21–23]. Furthermore, a transformation towards the orthorhombic seifertite structure (*Pbcn*) at ∼35 GPa has been found [21–24]. These studies provide evidence that, by using cristobalite as starting material, seifertite not only can form at lower pressures than expected from its thermodynamic equilibrium at ∼80 GPa [25,26] but also bypasses the thermodynamically favorable stishovite and CaCl$_2$ polymorphs. Interestingly, the transition of cristobalite X-I to seifertite was not observed in diamond anvil cell (DAC) experiments where α-cristobalite was compressed up to 80 GPa in a pressure-transmitting medium (PTM) [27]. These findings may indicate that these high-pressure phase transitions are dependent on the stress conditions during compression. It was further suggested that a change in pressure conditions, e.g., overpressurization, leads to a shift in the transition pressure from α-cristobalite to cristobalite II and cristobalite X-I [27,28]. This effect was experimentally demonstrated in a DAC up to a pressure of 15 GPa by increasing the compression of the diamond anvils instantaneously and thus leading to an extremely fast pressurization. Nonetheless, no systematic study has ever been conducted to investigate the relation of overpressurization on phase transitions of α-cristobalite. In this x-ray diffraction study, we used the dynamic diamond anvil cell (dDAC) to investigate the high-pressure behavior of single crystal and polycrystalline α-cristobalite and the formation of its high-pressure polymorphs at variable compression rates.

II. MATERIAL AND METHODS

α-Cristobalite was synthesized from fused silica (Goddfellow Cambridge Ltd.) in a high-temperature furnace (Carbolite
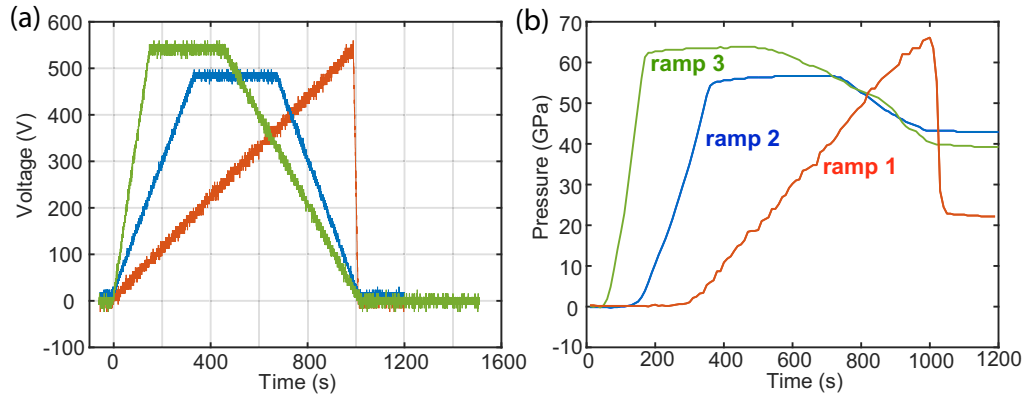
*schoelmerich1@llnl.gov

FIG. 1. (a) Example of three different waveform voltage profiles and (b) obtained pressures (GPa) resulting from indicated waveforms within the dDAC as a function of time (s).

Gero GmbH & Co. KG) at the Goethe University Frankfurt, Germany. Fused silica disks (500 μm thick and 2 cm long) were placed in the furnace at ambient pressure and maximum temperatures of 1550 °C for 24 h. Subsequently, samples were rapidly quenched by dropping the disks into water at the cold end of the furnace. The annealing procedure allowed the growth of α-cristobalite crystals of up to ~215 μm in linear dimension. The product was probed by μ-Raman spectroscopy to verify the cristobalite structure (Fig. S1 in the Supplemental Material [29]). Single crystal α-cristobalite pieces were cut and polished to ~15 μm thick disks along the growth direction. Furthermore, some α-cristobalite pieces were crushed and ground in a Zr mortar under acetone, to obtain a fine powder. The product was mixed with ~10 wt. % gold powder (Sigma Aldrich, 326 585), which was used as a pressure standard. Both single crystals and powders were loaded into a circular hole laser drilled into preindented rhenium gaskets. The gaskets were placed between 200 μm culet diamonds of symmetric DACs, enabling pressures of up to 106 GPa. Single crystals were loaded with Ne as a pressure transmitting medium, using a gas loading system installed at the Extreme Conditions Science Infrastructure (ECSI) at PETRA III of the Deutsches Elektronen-Synchrotron (DESY), Hamburg Germany. The DAC loaded with powder or single crystal cristobalite as a starting material was compressed along predefined compression ramps by means of a piezo actuator in the dDAC [30,31] (Fig. 1). Eight ramps were

performed to investigate the effect of different compression and decompression rates on the lattice response of α-cristobalite (Table I). X-ray diffraction was collected during compression by LAMBDA GaAs 2M detectors [32]. The photon energy was tuned to 25.6 keV for the experiments while the x-ray beam was focused through a compound refractive lens system to 8(h) 2(v) μm^2 FWHM. Sample to detector distance, detector tilt, and rotation were calibrated using a Cr_2O_3 (NIST 647b) standard and the DIOPTAS software [33]. Diffraction peaks on both detectors covered a 2θ range of 10° to 22°, which was sufficient to record the (111), (200), and (220) Bragg reflections of the Au pressure calibrant to the maximum pressure of the experiments. Furthermore, the 2θ range was sufficient to record major Bragg reflections of α-cristobalite, cristobalite II, cristobalite X-I, and seifertite. Data were subsequently integrated using the customized beamline software "P02 Processing Tool" in order to produce contour plots, facilitating a quick overview of the experiment. Integrated diffraction patterns were read into a Matlab script and filtered in an automated routine using the Savitzky-Golay function [34] (Fig. 2). We used Savitzky-Golay filtering to improve the signal/noise ratio, the reliability, and the speed of the Matlab routine. From the 2θ position of the smoothed diffraction peaks, Au as well as cristobalite reflections were fitted using a Gaussian function and subsequently indexed. Pressure of the sample was estimated from the (111), (200), and (220) Bragg reflections of the Au employing published

TABLE I. Summary of the experimental conditions of this study.

Run	Sample	P_{start} (GPa)	P_{max} (GPa)	Compression rate (GPa/s)	P_{end} (GPa)	Decompression rate (GPa/s)	End product
Run1	powder	0	69	0.07	21	0.96	Sft
Run2	powder	0	73	0.02	73	N/A[a]	Sft
Run3	powder	18	106	0.25	17	1.18	Sft
Run4	powder	0	57	0.17	43	0.05	Sft
Run5	powder	0	63	0.41	40	0.05	Sft
Run6	powder	0	92	0.19	41	0.03	Sft
Run7	single crystal	14	82	0.07	21	3.11	CXI
Run8	single crystal	21	31	0.01	31	N/A[a]	CXI

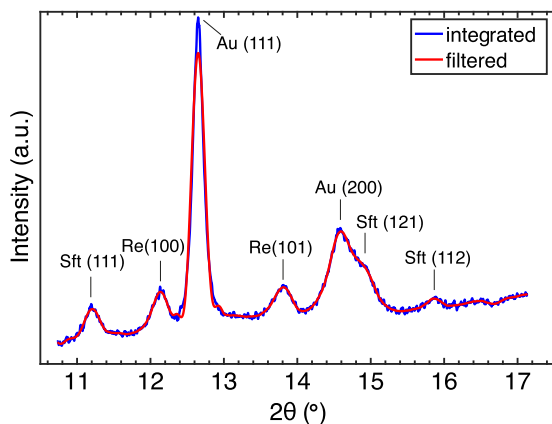[a]Diamonds broke; Sft = seifertite; CXI = cristobalite X-I.

FIG. 2. Diffraction pattern (run1) at 69 GPa. The blue line shows the integrated diffraction pattern obtained from DIOPTAS; the red line displays the lineout derived with the Savitzky-Golay filter. Shown are the Bragg reflections of seifertite (Sft), Au, and Re.

FIG. 3. Pressure as a function of compression rate for different dDAC runs using powder α-cristobalite as a starting material. Shown are the different high-pressure polymorphs of α-cristobalite: cristobalite II (CII), cristobalite X-I (CXI), and seifertite (sft). Dashed lines indicate approximate phase change pressures. The uncertainty in pressure determination for run3, run4, run5, and run6 is ~0.5 GPa, calculated from the minimal separable peak distance of the XRD pattern. For run1 and run2 the error is accounted to be around ~2.5 GPa due to the pressure uncertainties of the Au calibrant at low compression rates.

equation of state parameters [35]. The error in pressure is calculated from the minimal separable peak distance determined from the angular resolution of the detector (0.05° in 2θ). In agreement to a recent dDAC study [36], we found that the pressure obtained from the Au standard at slow compression rates was increasingly underestimated by 1–2.5 GPa at pressures above 35 GPa compared to the pressure determined from the volume of the sample using the known equation of state of seifertite [21] (Fig. S2 in the Supplemental Material [37]).

It has to be noted, however, that these pressure deviations were not observed for cristobalite II, cristobalite X-I, or for any runs using single crystals in a PTM, which is in agreement with [36]. Hence, the XRD patterns of the experiments using single crystals in a PTM as starting material (run7 and run8) and the Au pressure standard were used to calculate unit cell parameters of cristobalite X-I as a function of pressure.

III. RESULTS AND DISCUSSION

Throughout compression of all powder samples, the emergence of Bragg reflections corresponding to the α-cristobalite and its high-pressure polymorphs were observed, demonstrating the well known phase transition sequence of α-cristobalite $\rightarrow$ cristobalite II $\rightarrow$ cristobalite X-I $\rightarrow$ seifertite. The onset pressures of the individual α-cristobalite polymorph phase transitions were investigated under different compression rates (Table I). The phase transformation of α-cristobalite into cristobalite II was observed at pressures between 0.5–1 GPa in all experimental runs, regardless of the compression rate. The first appearance of cristobalite X-I Bragg reflections was detected between ~5–7 GPa for the slow compression rate runs (run1 and run2), ~7–9 GPa for the moderate runs (run4 and run6), and at ~11 GPa for the fast run (run5). For run3, the initial pressure in the cell had already reached ~18 GPa at the first XRD measurement and only the cristobalite X-I structure was observed. First seifertite Bragg reflections were detected between ~23–28 GPa for the slow runs (run1 and run2), ~28–31 GPa for the moderate runs (run4 and run6), and ~32–35 GPa for the fast runs (run3 and run5).
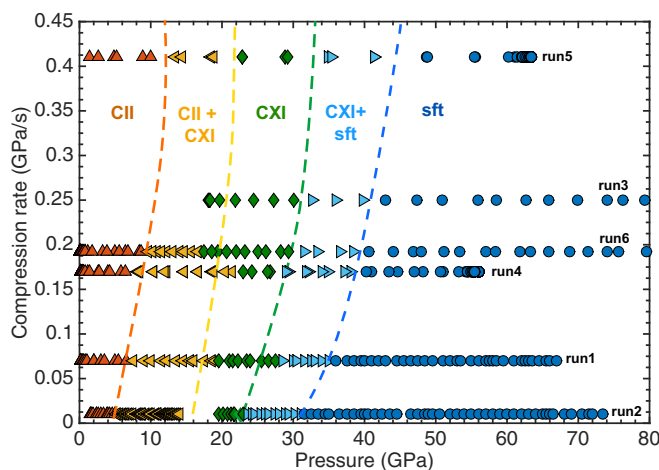
All experiments record a homogeneous phase transition behavior with structural mixtures of α-cristobalite + cristobalite II, cristobalite II + cristobalite X-I, and cristobalite X-I + seifertite in a single x-ray pattern. No back transformation to a low pressure phase could be observed at decompression in all experimental runs (Table I). Regardless of decompression rate, the end product of all powder loaded experimental runs were indexed to the seifertite structure in the explored pressure range.

Figure 3 depicts a comparative summary of the dDAC results from powder loaded runs showing the structural high-pressure response of α-cristobalite polymorphs with regard to the compression rate. The pressure onsets of the phase transformations systematically shift to higher pressures with increasing compression rate. Only the pressure onset of the phase transformation of α-cristobalite towards cristobalite II does not exhibit a clear correlation between compression rate and phase transformation. It has to be noted that the uncertainty of the pressure determination from the Au standard is ~0.5 GPa, hence it is comparable to the pressure range of the α-cristobalite $\rightarrow$ cristobalite II transition itself, preventing a conclusive correlation. Previous experimental studies have shown that an instantaneous overpressurization in a DAC can shift the phase transitions α-cristobalite, cristobalite II and cristobalite X-I to higher pressures [27,28]. Other dynamic compression studies on SiO$_2$ using membrane DACs, gas guns, or optical lasers have also found that fast compression rates can shift or even hinder high pressure phase transitions [38–41]. It was reported, for instance, that by using crystalline SiO$_2$ (α-quartz) as the starting material in a membrane DAC, the high pressure phase transition α-quartz $\rightarrow$ stishovite shifted towards pressures of up to 18–38 GPa [38] when compressed rapidly, much higher than expected from its
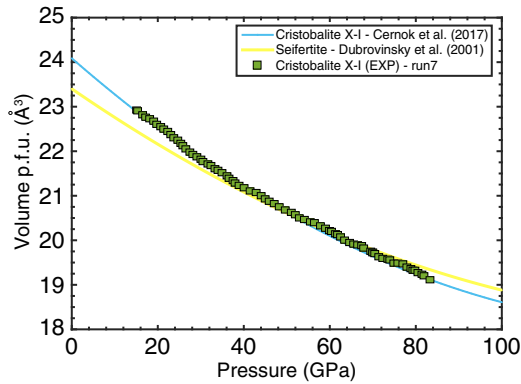
FIG. 4. Molecular volume per formula unit of cristobalite X-I as a function of pressure. Shown are experimental results of experiment run7 with a compression rate of 0.07 GPa/s. Solid lines indicate cristobalite X-I and seifertite data from previous works. The experimental data of this work are in excellent agreement with the cristobalite X-I fit of Ref. [27] at similar compression. The uncertainty in pressure determination is ~0.5 GPa and that of the unit cell volumes is ~0.02 $Å^3$.

steady state equilibrium transition pressure (~7 GPa) [2,8]. In another study, high-pressure phase transitions were not observed when stishovite was used as starting material in a laser-induced compression experiment [41]. Previous works suggested that rapidly compressed solids depend strongly on the strain rate of the compression, and consequently, higher transition pressures can be achieved through higher strain-rate drives [42,43]. However, shear stresses in samples can also lead to a lowering of phase transition boundaries from the hydrostatically determined values in fast-compression experiments [44]. Even though the compression rates in our study are comparably lower than most high-drive dDAC or shock compression experiments, a clear shift towards higher pressures with increasing compression rates can be observed, suggesting that the mechanism that α-cristobalite adopts during compression depends strongly on the stress conditions. In nonhydrostatic experiments, that is without any PTM using powders as starting material, we observe the α-cristobalite → cristobalite II → cristobalite X-I → seifertite phase transition sequence. Here grain interaction within the powder samples are most likely the major contributor to a nonhydrostatic environment [27].

In order to verify if the observed transitions are dependent on stress conditions within the sample, two quasihydrostatic experiments with single-crystal α-cristobalite in Ne as PTM were additionally conducted (Table I). The Bragg reflections

observed in run7 between 14 and 82 GPa can be indexed to the cristobalite X-I structure. There is no indication of a structural change in the explored pressure range. A third order Birch-Murnaghan equation of state [45] was fitted to the obtained *P-V* data (Fig. 4), yielding $V_0 = 195.43(25)$ $Å^3$ and $K_0 = 214(2)$ GPa with fixed $K' = 4$. Upon decompression to 21 GPa, no transition to a lower pressure SiO_2 polymorph was observed. This observation and the obtained EOS are in good agreement with a recent steady state DAC study, in which cristobalite X-I was shown to be stable at pressure of up to ~80 GPa under quasihydrostatic conditions [27]. Since the compression rates of experimental runs run7 and run8 are very low (0.07 and 0.01 GPa/s, respectively), it can be assumed that the results are comparable to static compression experiments. It was suggested that the relative low bulk modulus of cristobalite X-I can be associated with the significant amount of only partially occupied octahedra in the cristobalite X-I structure [27]. Our results also agree with theoretical molecular dynamic work, showing a strong dependence of the phase transition of cristobalite X-I to seifertite to hydrostatic conditions [46].

IV. CONCLUSIONS

We have collected continuous x-ray-diffraction data of the high pressure phase transition of α-cristobalite in a dynamically driven diamond anvil cell. We observed the high-pressure phase transitions from α-cristobalite to cristobalite II, cristobalite X-I, and seifertite in all experiments using powders as a starting material. We showed that the onset of the high-pressure phase transitions in α-cristobalite is sensitive to the compression rates explored in this study. No phase transition from cristobalite X-I to seifertite was observed when using single crystals in a PTM, suggesting a strong dependence on stress conditions within the sample during the experiments [47].

[1] L. Coes, A new dense crystalline silica, Science **118**, 131 (1953).

[2] S. Stishov and S. Popova, A new dense modification of silica, Geochemistry **10**, 923 (1961).

[3] S. Kitahara and G. Kennedy, The quartz-coesite transition, J. Geophys. Res. **69**, 5395 (1964).

[4] R. E. Cohen, Calculation of elasticity and high pressure instabilities in corundum and stishovite with the potential induced breathing model, Geophys. Res. Lett. **14**, 37 (1987).

[5] Y. Tsuchida and T. Yagi, A new, post-stishovite high pressure polymorph of silica, Nature (London) **340**, 217 (1989).

[6] K. J. Kingma, R. E. Cohen, R. J. Hemley, and H.-k. Mao, Transformation of stishovite to a denser phase at lower-mantle pressures, Nature (London) **374**, 243 (1995).

[7] D. Andrault, G. Fiquet, F. Guyot, and M. Hanfland, Pressure-induced Landau-type transition in stishovite, Science **282**, 720 (1998).

[8] V. P. Dmitriev, P. Tolédano, V. I. Torgashev, and E. K. H. Salje, Theory of reconstructive phase transitions between SiO_2 polymorphs, Phys. Rev. B **58**, 11911 (1998).

[9] R. Hemley, J. Shu, M. Carpenter, J. Hu, H. Mao, and K. Kingma, Strain/order parameter coupling in the ferroelastic transition in dense SiO_2, Solid State Commun. **114**, 527 (2000).

[10] J. K. Wicks and T. S. Duffy, Crystal structures of minerals in the lower mantle, Deep Earth: Phys. Chem. Lower Mantle Core **217**, 69 (2016).

[11] N. Sun, W. Shi, Z. Mao, C. Zhou, and V. B. Prakapenka, High pressure-temperature study on the thermal equations of state of seifertite and $CaCl_2$-type SiO_2, J. Geophys. Res.: Solid Earth **124**, 12620 (2019).

[12] A. V. Valkenburg, Jr. and B. Buie, Octahedral cristobalite with quartz paramorphs from Ellora caves, Hyderabad state, India, Am. Mineralog.t: J. Earth Planetary Mater. **30**, 526 (1945).

[13] P. Baxter, C. Bonadonna, R. Dupree, V. Hards, S. Kohn, M. Murphy, A. Nichols, R. Nicholson, G. Norton, A. Searl *et al.*, Cristobalite in volcanic ash of the Soufrière Hills volcano, Montserrat, British West Indies, Science **283**, 1142 (1999).

[14] C. J. Horwell, B. J. Williamson, E. W. Llewellin, D. E. Damby, and J. S. Le Blond, The nature and formation of cristobalite at the Soufrière Hills volcano, Montserrat: Implications for the petrology and stability of silicic lava domes, Bull. Volcanol. **75**, 696 (2013).

[15] A. J. Brearley, R. H. Jones, and J. Papike, Chondritic meteorites, Planet. Mater. **36**, C1 (1998).

[16] I. Weber, A. Greshake, and A. Bischoff, Low-cristobalite in the Martian meteorite Zagami, Lunar Planet. Sci. Conf. **31**, 1342 (2000).

[17] A. El Goresy, P. Dera, T. G. Sharp, C. T. Prewitt, M. Chen, L. Dubrovinsky, B. Wopenka, N. Z. Boctor, and R. J. Hemley, Seifertite, a dense orthorhombic polymorph of silica from the Martian meteorites Shergotty and Zagami, Eur. J. Mineral. **20**, 523 (2008).

[18] M. Miyahara, S. Kaneko, E. Ohtani, T. Sakai, T. Nagase, M. Kayama, H. Nishido, and N. Hirao, Discovery of seifertite in a shocked lunar meteorite, Nat. Commun. **4**, 1737 (2013).

[19] U. W. Bläß, Shock-induced formation mechanism of seifertite in shergottites, Phys. Chem. Miner. **40**, 425 (2013).

[20] T. Sharp, A. El Goresy, B. Wopenka, and M. Chen, A post-stishovite SiO_2 polymorph in the meteorite Shergotty: Implications for impact events, Science **284**, 1511 (1999).

[21] L. Dubrovinsky, N. Dubrovinskaia, S. Saxena, F. Tutti, S. Rekhi, T. Le Bihan, G. Shen, and J. Hu, Pressure-induced transformations of cristobalite, Chem. Phys. Lett. **333**, 264 (2001).

[22] V. Prokopenko, L. Dubrovinsky, V. Dmitriev, and H.-P. Weber, In situ characterization of phase transitions in cristobalite under high pressure by Raman spectroscopy and x-ray diffraction, J. Alloys Compd. **327**, 87 (2001).

[23] V. Prakapenka, G. Shen, L. Dubrovinsky, M. Rivers, and S. Sutton, High pressure induced phase transformation of SiO_2 and GeO_2: Difference and similarity, J. Phys. Chem. Solids **65**, 1537 (2004).

[24] N. A. Dubrovinskaia, L. S. Dubrovinsky, S. K. Saxena, F. Tutti, S. Rekhi, and T. Le Bihan, Direct transition from cristobalite to post-stishovite α-PbO_2-like silica phase, Eur. J. Mineral. **13**, 479 (2001).

[25] L. Dubrovinsky, S. Saxena, P. Lazor, R. Ahuja, O. Eriksson, J. Wills, and B. Johansson, Experimental and theoretical identification of a new high-pressure phase of silica, Nature (London) **388**, 362 (1997).

[26] B. Grocholski, S.-H. Shim, and V. Prakapenka, Stability, metastability, and elastic properties of a dense silica polymorph, seifertite, J. Geophys. Res.: Solid Earth **118**, 4745 (2013).

[27] A. Černok, K. Marquardt, R. Caracas, E. Bykova, G. Habler, H.-P. Liermann, M. Hanfland, M. Mezouar, E. Bobocioiu, and L. Dubrovinsky, Compressional pathways of α-cristobalite, structure of cristobalite X-I, and towards the understanding of seifertite formation, Nat. Commun. **8**, 15647 (2017).

[28] P. Dera, J. D. Lazarz, V. B. Prakapenka, M. Barkley, and R. T. Downs, New insights into the high-pressure polymorphism of SiO_2 cristobalite, Phys. Chem. Miner. **38**, 517 (2011).

[29] See Supplemental Material at http://link.aps.org/supplemental/10.1103/PhysRevB.105.064109 for further details on Raman spectroscopy results including the fused silica and cristobalite peak determination.

[30] W. J. Evans, C.-S. Yoo, G. W. Lee, H. Cynn, M. J. Lipp, and K. Visbeck, Dynamic diamond anvil cell (DDAC): A novel device for studying the dynamic-pressure properties of materials, Rev. Sci. Instrum. **78**, 073904 (2007).

[31] Z. Jenei, H. Liermann, R. Husband, A. Méndez, D. Pennicard, H. Marquardt, E. OBannon, A. Pakhomova, Z. Konopkova, K. Glazyrin *et al.*, New dynamic diamond anvil cells for tera-pascal per second fast compression x-ray diffraction experiments, Rev. Sci. Instrum. **90**, 065114 (2019).

[32] D. Pennicard, S. Smoljanin, F. Pithan, M. Sarajlic, A. Rothkirch, Y. Yu, H. Liermann, W. Morgenroth, B. Winkler, Z. Jenei *et al.*, LAMBDA 2M GaAsA multi-megapixel hard x-ray detector for synchrotrons, J. Instrum. **13**, C01026 (2018).

[33] C. Prescher and V. B. Prakapenka, DIOPTAS: A program for reduction of two-dimensional x-ray diffraction data and data exploration, High Press. Res. **35**, 223 (2015).

[34] A. Savitzky and M. J. Golay, Smoothing and differentiation of data by simplified least squares procedures, Anal. Chem. **36**, 1627 (1964).

[35] O. L. Anderson, D. G. Isaak, and S. Yamamoto, Anharmonicity and the equation of state for gold, J. Appl. Phys. **65**, 1534 (1989).

[36] R. J. Husband, E. F. OBannon, H.-P. Liermann, M. J. Lipp, A. S. Méndez, Z. Konôpková, E. E. McBride, W. J. Evans, and Z. Jenei, Compression-rate dependence of pressure-induced phase transitions in Bi, Sci. Rep. **11**, 14859 (2021).

[37] See Supplemental Material at http://link.aps.org/supplemental/10.1103/PhysRevB.105.064109 for further details on the pressure comparison between the Au calibrant and the published equation of state of seifertite.

[38] E.-R. Carl, U. Mansfeld, H.-P. Liermann, A. Danilewsky, F. Langenhorst, L. Ehm, G. Trullenque, and T. Kenkmann, High-pressure phase transitions of α-quartz under nonhydrostatic dynamic conditions: A reconnaissance study at PETRA III, Meteor. Planet. Sci. **52**, 1465 (2017).

[39] E.-R. Carl, H.-P. Liermann, L. Ehm, A. Danilewsky, and T. Kenkmann, Phase transitions of α-quartz at elevated temperatures under dynamic compression using a membrane-driven diamond anvil cell: Clues to impact cratering? Meteor. Planet. Sci. **53**, 1687 (2018).

[40] S. J. Tracy, S. J. Turneaure, and T. S. Duffy, *In Situ* X-ray Diffraction of Shock-Compressed Fused Silica, Phys. Rev. Lett. **120**, 135702 (2018).

[41] M. O. Schoelmerich, T. Tschentscher, S. Bhat, C. A. Bolme, E. Cunningham, R. Farla, E. Galtier, A. E. Gleason, M. Harmand, Y. Inubushi *et al.*, Evidence of shock-compressed stishovite above 300 GPa, Sci. Rep. **10**, 10197 (2020).

[42] R. F. Smith, J. H. Eggert, M. D. Saculla, A. F. Jankowski, M. Bastea, D. G. Hicks, and G. W. Collins, Ultrafast Dynamic Compression Technique to Study the Kinetics of Phase Transformations in Bismuth, Phys. Rev. Lett. **101**, 065701 (2008).

[43] R. Smith, J. Eggert, D. Swift, J. Wang, T. S. Duffy, D. Braun, R. Rudd, D. Reisman, J.-P. Davis, M. Knudson *et al.*, Time-dependence of the alpha to epsilon phase transformation in iron, J. Appl. Phys. **114**, 223507 (2013).

[44] E. E. McBride, A. Krygier, A. Ehnes, E. Galtier, M. Harmand, Z. Konôpková, H. Lee, H.-P. Liermann, B. Nagler, A. Pelka *et al.*, Phase transition lowering in dynamically compressed silicon, Nat. Phys. **15**, 89 (2019).

[45] O. L. Anderson, O. L. Anderson *et al.*, *Equations of State of Solids for Geophysics and Ceramic Science*, Vol. 31 (Oxford University Press on Demand, Oxford, 1995).

[46] D. Donadio, R. Martoňák, P. Raiteri, and M. Parrinello, Influence of Temperature and Anisotropic Pressure on the Phase Transitions in α-Cristobalite, Phys. Rev. Lett. **100**, 165502 (2008).

[47] See Supplemental Material at http://link.aps.org/supplemental/10.1103/PhysRevB.105.064109 for information regarding sample characterization and an overall view of the presented experiments showing the reproducibility and uncertainties of the pressure standard in our observations.